Biomedical Engineering Advances 9 (2025) 100154

Contents lists available at ScienceDirect

Biomedical Engineering Advances

journal homepage: www.journals.elsevier.com/biomedical-engineering-advances

# Translation of single channel electro encephalic signals into limb motion

A.B.R. Lara [a], Oscar E. Ruiz [b], L.O. Araujo Junior [a], F.P. Bhering [a],*

[a] *Centro Federal de Educação Tecnológica de Minas Gerais, MG, Brazil*
[b] *Universidad EAFIT, Laboratorio de CAD CAM CAE, Medellin, Colombia*

ARTICLE INFO

*Keywords:*
Neuroprothesis
Brain–computer interface
Electroencephalography

ABSTRACT

Neural prostheses (NPs) are devices that can translate brainwaves into motion. The non-invasive multi-channel headset used in the study of Brain–Computer Interface (BCI) systems for the development of NPs, presents high resolution in data collection, but also presents high computing expenses and hardware costs. To overcome the barrier of the costs and present an accessible technology for these studies, this manuscript presents the implementation of a method that uses a single-channel headset to sample the Electro Encephalo Graph (EEG) wave. The headset provides 8 individual brain waves (delta, theta, low alpha, high alpha, low beta, high beta, low gamma, mid gamma), operating in their characteristic frequency intervals. A Multi-layer Perceptron (MLP) was trained with the Alpha and Beta waves (4 signals), reaching a $73,9\%$ accuracy rate for detecting the movement (open/close) of the subject's right hand. The conclusion on the subject hand status is fed into a kinematic (Denavit Hartenberg) model of the hand, to simulate the opening/ closing of a robotic hand. The results confirm the usability of the single-channel headset to extract information from the motor cortex for the development of cheaper and more accessible NPs. The advantages of this method are: (a) lower hardware expense and (b) lower computing load. The disadvantages of our approach lie in the time needed for the 15 s to react to the real-time patient brain signal and to produce the Open/Close command to the Neural Prosthesis. Future endeavors include the online usage of the trained NN by the subject. An additional interest domain is the usage of intention-of-movement brain waves for forecasting.

## 1. Introduction

Electroencephalography (EEG) is a method to measure the electrical activity of the brain. The division of this electrical activity into specific frequencies originates from the so-called brainwaves. Brain waves are patterns of neural activity, and are the result of interactions between the firing of neurons, these are a very special type of signal, that is, the brain is the processing center of the body, where commands are produced and stimuli interpreted, all the functionalities of the body begin in the brain. By analyzing these signals it is possible to extract information such as visual and motor stimuli, as well as information on brain diseases.

In detections of clinical cases, such as Alzheimer's disease, it is necessary to use a dense array of EEG, that is, a sensor network with many channels (an electrode capturing brainwave activity is called an EEG channel), thus doing a better job avoiding the loss of any crucial data. Medical cases need higher-resolution EEG systems (larger sensor networks) to get the job done. Some other applications developed using brainwaves are neurorehabilitation, functional recovery, communication tools, and prosthetic control for severe disabilities, etc. For each application, it is necessary to analyze a specific frequency range and use different methods to extract the desired characteristics of the signal.

Brain–computer Interface is a system that makes a direct communication between brain and machine, had its first appearance in the 1970s [1]. BCI systems are developed using EEG or other metrics to measure brain activity, or even using a hybrid device that uses the EEG signals along with EMG, EOG, or other types of biophysiological signals. In addition to the type of signal used to develop a BCI or a hybrid BCI, there are kinds of BCI systems that require neurosurgery to be used, the so-called invasive and partially invasive BCIs, differentiating itself by the place where the electrode, that capture the brain activity, is fixed, also there are some that are more convenient options for the users, these are BCIs that use headsets with single or multi-channels and dry electrodes on the scalp, [2].

A high resolution of recorded data is essential for clinical case detection, but it is not a law for all fields of brainwave research. The main objective of this article is to propose an inexpensive alternative to extract information from the motor cortex, with lower computational expenses, in view of the future studies and development of NPs.

* Corresponding author.
*E-mail address:* fabianobhering@cefetmg.br (F.P. Bhering).

https://doi.org/10.1016/j.bea.2025.100154
Received 30 October 2024; Received in revised form 11 February 2025; Accepted 8 March 2025
Available online 23 March 2025

**Table 1**
Glossary.

| | | |
|---|---|---|
| $NP$ | : | Neuroprosthesis, a prosthesis used to improve some function impaired by the nervous system disability. |
| $EEG$ | : | Electroencephalography (EEG) is an electrophysiological monitoring method that is used to record the electrical activity of the brain. |
| $MEG$ | : | Magnetoencephalography, is a technique for mapping the activity of the human brain by detecting the magnetic field produced by electric currents that naturally exist in the brain. |
| $MIR$ | : | Magnetic resonance imaging, is an imaging technique that uses strong magnetic fields, radio waves and field gradients to generate images of the organs in the body. |
| $fMIR$ | : | Functional magnetic resonance imaging, is a specific technique for the use of magnetic resonance imaging capable of detecting variations in blood flow in response to neural activity. |
| $BCI$ | : | Brain-Computer Interface (BCI), it is a hardware and software communications system that permits catch the brain waves. |
| $ASIC$ | : | Application-Specific Integrated Circuit (ASIC) is a kind of integrated circuit that is specially built for a specific application or purpose. |
| $TGAM$ | : | ThinkGear ASIC Module (TGAM)is the NeuroSky's primary brainwave sensor, responsible for processing the brain activity. |
| $eSense$ | : | An algorithm developed by NeuroSky to measure mental states like, Attention and Meditation levels. |
| $NN$ | : | Neural Network (NN) is based on a collection of connected nodes called artificial neurons which loosely model the neurons in a biological brain. |
| $WT$ | : | Wavelet Transform (WT), a mathematical tool for signal analysis and processing. |
| $FSVM$ | : | Fuzzy Support Vector Machine (FSVM), a variant of SVM that incorporates fuzzy logic for classification. |
| $MLP$ | : | Multilayer Perceptron (MLP), a class of feedforward artificial neural network that consists of multiple layers of nodes, each layer fully connected to the next one. |
| $BFGS$ | : | Broyden–Fletcher–Goldfarb–Shanno (BFGS) algorithm, a Quasi-Newton method for optimizing neural network training by approximating the Hessian matrix. |
| $MA$ | : | Moving Average (MA), a statistical method to smooth data by calculating averages over subsets, highlighting trends. |
| $FIR$ | : | Finite Impulse Response (FIR) filter, a digital filter with a finite response to an input signal, commonly used for signal processing. |

The paper is structured as follows. The second section will relate techniques and equipment used in the study of brain waves. The next section has a system exposition, robot development, a quick brainwave discussion, and patient preparation which shows the steps to follow to recreate the same datasets that were used in this research, the equipment usage exposes other requirements to replicate the experiment and data processing shows the operation of the entire system. Finally, the results and discussion section contains the results of the case study, focused on the data used, the filtering stage, and the classifier accuracy. The last section, the conclusion, presents the contribution and future work.

## 2. Literature review

Some authors have presented state-of-the-art technologies and applications for EEG-based brain–computer interfaces. [3] describe a Noninvasive EEG-Based Intelligent Mobile Robots. It presents the general architecture and basic concepts, typical system types, and main research efforts on whole system design. In addition, relevant key techniques associated with brain–machine interfaces, control strategies, and robot intelligence are reviewed to elucidate the research progress of the overall system (see Table 1).

[4] explore among the different brain imaging techniques used to operate brain–computer interfaces (BCI) and electroencephalography (EEG) constitutes the preferred method of choice, due to its relatively low cost, ease of use, high temporal resolution, and non-invasiveness. In recent years, significant progress in wearable technologies and computational intelligence has greatly improved the performance and capabilities of EEG-based BCI (eBCI) and propelled their migration out of the laboratory and into real-world environments. This rapid translation constitutes a paradigm shift in human–machine interaction that will deeply transform industries shortly, including healthcare and wellbeing, entertainment, security, education, and marketing. In this contribution, state-of-the-art wearable biosensing is reviewed, focusing on developing novel electrode interfaces for long-term and non-invasive EEG monitoring. Commercially available EEG platforms are surveyed and a comparative analysis is presented based on the benefits and limitations they provide for eBCI development. Emerging applications in neuroscientific research and future trends related to the widespread implementation of eBCIs for medical and nonmedical uses are discussed.

[5] examines the various components of a BCI system, such as hardware, software, and signal processing algorithms. The paper concludes by highlighting some key challenges that still need to be addressed before widespread adoption can occur. By presenting an up-to-date assessment of the state-of-the-art in BCI technology, providing valuable insight into where this field is heading in terms of progress and innovation.

Other related techniques are:

**EEG-based BCI systems:** Some techniques that record brain activity are, EEG, MEG, MRI, and fMRI, each one works in a self-way. Among these techniques, EEG is widely used due to its relatively low cost, high temporal resolution, and convenience for users. Setting up an experiment with EEG can be done as easily as placing a headset on, while the other metrics need a bigger machine which results in a high cost [6]. For quicker, affordable, and accessible insights about brain function, with a tight temporal resolution, EEG is the method of choice.

**Multi-channels Headset:** Current studies of brainwaves are realized using this technology, a very used equipment in this field are the headsets from Emotiv™ with fourteen channels [7–10], also there are other used headsets with more channels [11–15], the number of channels allows record the brain activity with more resolution, the high resolution is essential to clinical conditions applications, such as discover brain diseases, to get a reliable result, it is necessary use a dense array of electrodes. In the use of the multi-channel headset, it is necessary at least one step more than using a single-channel headset, this step is used to reduce the amount of data recorded by the headset, selecting which channels are better to work, its main disadvantage is the high cost of the equipment.

**Neurosky headset:** Neurosky™ is a famous company that develops solutions with biophysiologic signals. The greatest part of its fame is due to the low costs of its products. Mindwave is a single-channel headset developed by Neurosky™ to developers, and researchers, it is a cheap tool that allows the capture and analysis the brain activity. Some researches were developed using the mind wave headset, in an application of mobility [16,17], Neuroprosthesis [18,19] and communication tools [20], although these researches were developed using levels of attention, meditation and the detect of the blink to create protocols and thus produce commands.

**Neural Network:** In the literature almost all research presents a different combination of tools and classifiers to extract the desired information from the EEG signal. The use of the FSVM [21], WT [22, 23], Genetic Algorithm [24], Convolutional neural network-based [25], and Deep Learning techniques ([26] are common tools used in the study of the brainwaves. One of the best classifiers used in those researches is Neural Network, it is an excellent tool that presents a higher accuracy rate, it is very flexible, has multi-classes and infinite architectures [27–29].

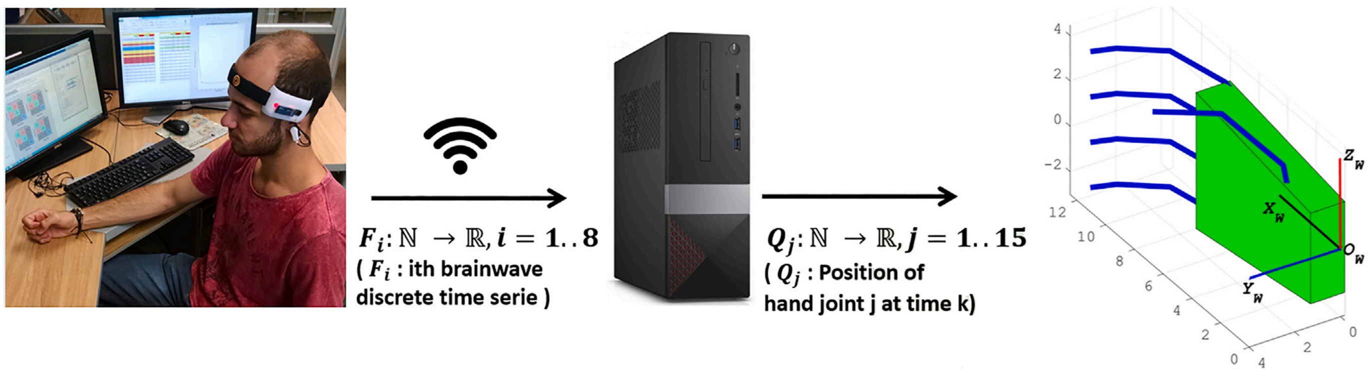


**Fig. 1.** System overview.

*2.1. Conclusions of the literature review and contributions of this work.*

There are not many solutions already made in the field of Neuroprosthesis (NP), but it is a field that is increasing in the aspect of studies and people who work with it. The current studies are focused on applications such as the classification of a specific movement, distinguishing different movements, and even distinguishing real movements from imaginary, all this information is contained in the motor cortex. These studies are performed with multi-channel headsets, which a good equipment, but have a high cost and computing expenses. To overcome this barrier, a single-channel headset by Neurosky™was used to perform studies on the motor cortex, aiming to extract the motion information and feed it into a robot to simulate the studied phenomenon, presenting then an alternative and inexpensive technology to study these signals.

## 3. Methodology

*3.1. System design*

In view of the aim of the present study, to use a single channel headset to collect information on the brain's motor system, the open/close of the subject's right hand, as an elementary movement to record the data. Using the Midflex headset by Neurosky™, the brain activity is sent via Bluetooth to a computer, where the brainwaves pass into a processing stage, the result of that stage is used as a command signal to produce a movement of the Denavit–Hartenberg (DH) robot. Fig. 1 shows a synthesized vision of the system. The BCI sends (via bluetooth) eight time series (Brainwaves) to a computer which process the data and change the robot position.

*3.2. Robot kinematics*

The DH convention arises to standardize the coordinate frames, it is a useful method which attaching reference frames to the joints of a robot manipulator. Using the homogeneous transformation matrices this convention allows describe the kinematics of the robot manipulators. The matrix DH convention, [30]:

$$C^i_{i-1} = \begin{pmatrix} cos(\Theta_i) & -cos(\alpha_i) * sin(\Theta_i) & sin(\alpha_i) * sin(\Theta_i) \\ sin(\Theta_i) & cos(\alpha_i) * cos(\Theta_i) & -sin(\alpha_i) * cos(\Theta_i) \\ 0 & sin(\alpha_i) & cos(\alpha_i) \end{pmatrix} \quad (1)$$

$$d^i_{i-1} = \begin{pmatrix} a_i * cos(\Theta_i) \\ a_i * sin(\Theta_i) \\ d_i \end{pmatrix} \quad (2)$$

$$T^i_{i-1} = \left( \begin{array}{ccc|c} & C^i_{i-1} & & d^i_{i-1} \\ \hline 0 & 0 & 0 & 1 \end{array} \right) \quad (3)$$

Replacing the matrices (1) (Rotation matrix) and (2) (Translation vector) in (3) (Homogeneous displacement matrix), shall result in a generic DH Displacement Matrix, this matrix describes all robot's kinematics to rotational and prismatic joints.

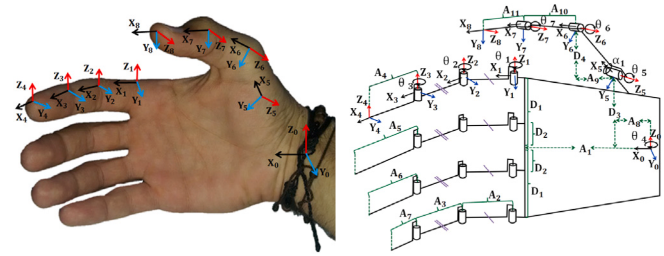

(a) Real hand with coordinate system (b) Hand knematic model

**Fig. 2.** Links coordinate system and joint parameters for Hand model.

The right-hand movement was selected for detailed analysis, along with the associated robot kinematics. As illustrated in Fig. 2(a), this movement provides a representative case for studying the system's behavior. The hand kinematic model, depicted in Fig. 2(b), was developed using the DH convention. Reference frames were systematically attached to each joint of the finger to establish a consistent and accurate representation of its motion.

Note that the hand is composed of fifteen joints. The finger's joints are rotational, that is, the joints only execute a rotational movement, so the variable that will be manipulated is an angle, in this case, the angle around the $Z_i$ axis. A reference frame was attached at the base of the hand, the other frames were attached following the order of the index finger until the thumb.

The only finger that will realize a distinguished movement is the thumb, the remaining will execute the same movement, distinguishing themselves by the last $a_i$ parameter of each finger that represents the real difference of the size among them and by the $d_i$ parameter that set the vertical position of each one. The following parameters represent the variables of the joints provided by the hand kinematic model (Fig. 2(b)). Analyzing the parameters in Table 2, it is notable that the parameters of the thumb are a little different from the remaining, which explains why the thumb realizes a different movement from the other fingers. Which makes the thumb perform a vertical movement while the remaining realize a horizontal movement are the parameter $\alpha_1$, which represents a rotation of 90° in anticlockwise around $X_5$ axis, and $\theta_4$, which in this case, represent a fixed rotation between $O_5$ and $O_0$ around $Z_0$.

The DH model of the robot was implemented in MATLAB™ using the parameters listed in Table 2. The system involves six distinct angles to be manipulated: three correspond to the thumb, while the remaining are the angles of the other fingers. As previously mentioned, all fingers are programmed to execute the same movement.

Inserting predefined initial and final joint angles, and the parameters of the links into MATLAB™ code the DH robot is created. Fig.

**Table 2**
Fingers parameters. $a_i$: size of the model's link. $d_i$: vertical distance between $O_0$ and $O_i$. $\alpha_1$: rotation angle around $X_5$. $\theta_i$: rotation angle around $Z_i$.

| Joint $i$ | $\theta_i$ | $d_i$ | $a_i$ | $\alpha_i$ |
|---|---|---|---|---|
| 1 | 0 | $D_1$ | $A_1$ | 0 |
| 2 | $\theta_1$ | 0 | $A_2$ | 0 |
| 3 | $\theta_2$ | 0 | $A_3$ | 0 |
| 4 | $\theta_3$ | 0 | $A_4$ | 0 |

(a) Index finger

| Joint $i$ | $\theta_i$ | $d_i$ | $a_i$ | $\alpha_i$ |
|---|---|---|---|---|
| 5 | 0 | $D_2$ | $A_1$ | 0 |
| 6 | $\theta_1$ | 0 | $A_2$ | 0 |
| 7 | $\theta_2$ | 0 | $A_3$ | 0 |
| 8 | $\theta_3$ | 0 | $A_5$ | 0 |

(b) Middle finger

| Joint $i$ | $\theta_i$ | $d_i$ | $a_i$ | $\alpha_i$ |
|---|---|---|---|---|
| 9 | 0 | $-D_2$ | $A_1$ | 0 |
| 10 | $\theta_1$ | 0 | $A_2$ | 0 |
| 11 | $\theta_2$ | 0 | $A_3$ | 0 |
| 12 | $\theta_3$ | 0 | $A_6$ | 0 |

(c) Ring finger

| Joint $i$ | $\theta_i$ | $d_i$ | $a_i$ | $\alpha_i$ |
|---|---|---|---|---|
| 13 | 0 | $-D_1$ | $A_1$ | 0 |
| 14 | $\theta_1$ | 0 | $A_2$ | 0 |
| 15 | $\theta_2$ | 0 | $A_3$ | 0 |
| 16 | $\theta_3$ | 0 | $A_7$ | 0 |

(d) Pinky

| Joint $i$ | $\theta_i$ | $d_i$ | $a_i$ | $\alpha_i$ |
|---|---|---|---|---|
| 17 | $\theta_4$ | $D_3$ | $A_8$ | $\alpha_1$ |
| 18 | $\theta_5$ | 0 | $A_9$ | 0 |
| 19 | $\theta_6$ | 0 | $A_{10}$ | 0 |
| 20 | $\theta_7$ | 0 | $A_{11}$ | 0 |

(e) Thumb

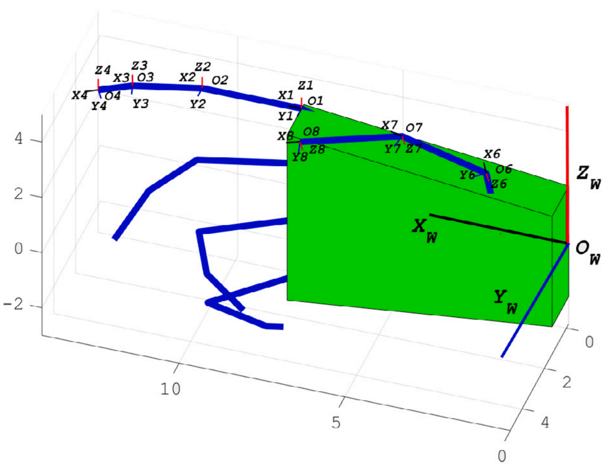


**Fig. 3.** Hand in DH representation.

**Table 3**
Brainwaves informations.

| Name | Frequency | Associated brain region and Intentions |
|---|---|---|
| Delta | $1-3\ Hz$ | Deeper regions such as the thalamus. |
| Theta | $4-7\ Hz$ | Hippocampus, memory. |
| Alpha | $8-12\ Hz$ | Motor cortex, motor intentions. |
| Beta | $13-30\ Hz$ | Motor cortex, motor intentions. |
| Gamma | $31-50\ Hz$ | Local neural circuits in cortex, motor intentions,auditory processing, and speech production. |

3 was generated by making an interpolation in $N$ steps between the initial and final angles and using a different step to plot each finger.

### 3.3. Brainwaves

Brainwaves are rhythmic or repetitive patterns of neural activity. They are generated within individual neurons or by the interactions between them. The synchronized activity of a large number of neurons can give rise to macroscopic oscillations, which can be observed in an EEG.

EEG activity always reflects the summation of the synchronous activity of thousands of neurons that have similar spatial orientation. EEG is the superposition of many elementary signals. The elemental frequencies of the human EEG waves are shown in Table 3.

The motor systems located at the motor cortex, produce a pattern of oscillations which can be recorded in a frequency of Alpha and Beta waves (8–30 Hz), this frequency range is called sensorimotor rhythms. When the motor system is activated can notice a reduction in Alpha and Beta waves, this event is called event-related synchronization/event-related desynchronization (ERS/ERD) [31,32]. For the phenomenon analyzed in this research, only the frequency of the sensorimotor rhythms will be used, because this is the frequency band that carries the movement information.

Current studies on sensorimotor rhythms are realized using multi-channel headsets, which have electrodes located at the motor cortex area. This strategy allows a better resolution in the record the cortex information, however, as it was said before, the brainwaves are a summation of millions of neurons firing, this characteristic allows recording the information of that specific area in some other, like in the forehead.

**Table 4**
Identification of Research Volunteers.

| Sex | Age | Motor disability | Contact with MindFlex (days) |
|---|---|---|---|
| Male | 22 | No | 60+ |

### 3.4. Preparation of patient/subject

The aim of this article is to present and validate a method through a human subject, providing all the necessary details to replicate this experiment and conduct future studies. The participant involved in this research is described in Table 4.

To ensure the reproducibility of the experiment, specific steps must be followed. The data recording process begins with the subject sitting down, wearing the headset, and turning it on. Once activated, the device starts capturing the subject's brain activity.

For dataset creation, three motor information were considered: (i) elementary movement, (ii) other body movements, and (iii) no movement.

Two datasets were generated. Dataset 1, illustrated in Fig. 4(a), consists of three recording sessions, each lasting ten minutes. Each session is dedicated exclusively to one type of motor information: the first session captures other body movements, the second session records only elementary movement, and the third session contains data exclusively from the no-movement condition. Dataset 2, shown in Fig. 4(b), consists of two sessions, each lasting two minutes: the first session includes a combination of other body movements and no movement, while the second session includes only elementary movement.

This structured approach ensures the segmentation and classification of motor activities, facilitating further analysis.

### 3.5. Equipment usage

To capture the brain activity was used the Mindflex headset by Neurosky™, demonstrated in Fig. 5. It is a headset with a forehead electrode used into Mindflex™, which is a PvP (player versus player) game in a physical platform with obstacles, that demand concentration and relaxing of the player to produce commands to win the game.

ThinkGear™, is the technology inside every NeuroSky™ product or partner product that enables the device to interface with the wearer's

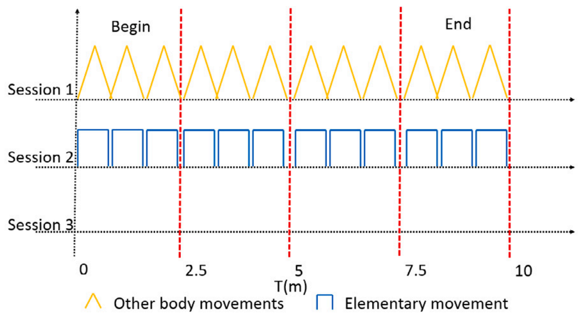


(a) Motor execution in each session of Dataset 1

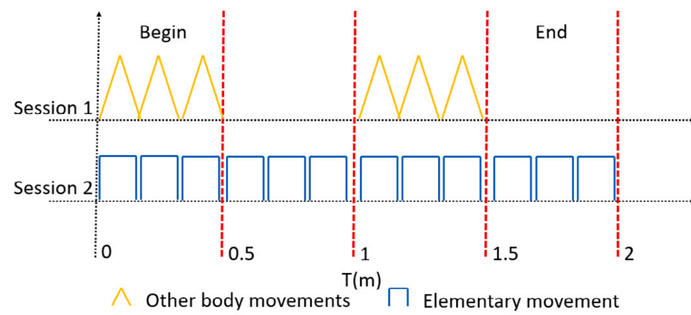


(b) Motor execution in each session of Dataset 2

**Fig. 4.** Motor execution in each session of Dataset 1 and Dataset 2.

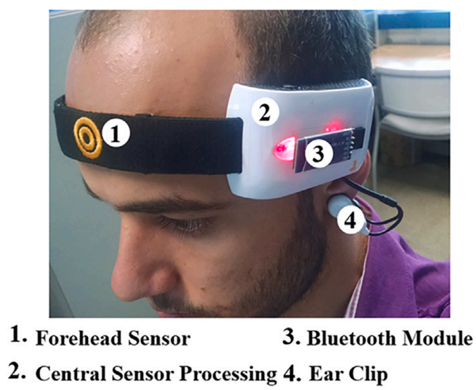


**Fig. 5.** Mindflex headset by Neurosky™.

**Table 6**
Position of robot joints at rest and disturbed state.

| $\theta_i$ | Rest State ($\theta_{r_1}$) | Disturb state ($\theta_{d_1}$) |
|---|---|---|
| $\theta_1$ | 0° | 45° |
| $\theta_2$ | 15° | 120° |
| $\theta_3$ | 15° | 30° |

(a) Table of the angular position of the four fingers in each state.

| $\theta_i$ | Rest State ($\theta_{r_2}$) | Disturb state ($\theta_{d_2}$) |
|---|---|---|
| $\theta_5$ | −80° | −75° |
| $\theta_6$ | 45° | 60° |
| $\theta_7$ | 30° | 90° |

(b) Table of the angular position of the thumb in each state.

**Table 5**
Experimental setup of used equipment.

| Parameters | Values |
|---|---|
| Equipment | Mindflex headset by Neurosky™ |
| Filter | Moving average filter |
| Filter length | 16 |
| Classifier | MLP |
| Training Algorithm | 'trainbfg' |
| Performance Algorithm | 'crossentropy' |
| Software | MATLAB™ |

brainwaves. It consists of three key components: a forehead sensor that detects brainwave activity, contact and reference points located on the ear pad to ensure proper signal acquisition, and an onboard chip that processes all the collected data.

Mindflex's platform communicates with the ThinkGear™ via radio frequency using the Neurosky's cryptography and does not allows access to the brain activity informations, cause of this, some people developed ways to export these informations to an other place. The technology used in this equipment was the Bluetooth module, which export the data.

Fig. 6 provides an overview of the system's processing pipeline. The ThinkGear ASIC Module (TGAM) process raw EEG data from the NeuroSky headset and transmits it via Bluetooth to a computer for further processing. The headset provides multiple output signals, including Signal Quality, Attention and Meditation levels, and a set of brainwave frequency bands: Delta, Theta, Low Alpha, High Alpha, Low Beta, High Beta, Low Gamma, and Mid Gamma. A summary of the parameters used in the experimental setup, along with their corresponding values, is provided in Table 5.

The headset sends through Bluetooth one packet per second at a rate of 9600 bps (bits per second). Each packet carries the updated information of the brain activity, which is recorded in a .txt document by an algorithm developed in C++.

The software selected to process the data recorded was MATLAB™, due to its Neural Network toolbox. The topology of NN used was the multi-layer perceptron (MLP). The training algorithm 'trainbfg'was used to allow a better generalization of the NN, that is, it can replicate the right classification for different datasets. As those datasets will receive the target information, the perform algorithm used was 'crossentropy'.

EEG data has many noises, even if the headset uses filters before sending the data, so it is necessary to use an extra filter to remove these noises, in this case, the moving average filter was selected to do this work because it is a good type of filter to be used in biophysiological signals. The length of the filter window is sixteen, this value was selected because it is a length that smooths the signal well without loss of information.

### 3.6. Data processing

Once the data has already been collected, they are imported into the MATLAB™, where the respective target is added in each sampled data and therefore they are grouped in sequence. Now the data follows the sequence of the flowchart passing through all stages, as presented in Fig. 7. After this first manipulation of the data, they are fed into a noise removal stage to reduce the noise and smoothing them to become the input of the Neural Network. The MLP was used as a pattern recognition NN, which separates the data into classes. The problem is that this type of NN cannot predict the position of the hand for each sample of brainwaves, it only classifies whether or not there is movement of the subject's right hand. To overcome this problem, the movements of the robot were limited ($Q_j(k)\, \mathbb{N} \rightarrow \theta_R, \theta_D$, where $\theta_R$ and $\theta_D$ are defined in Table 6), and a rest and disturbance state of the robot has been created. The resting state occurs when there is no movement of the right hand, while the disturbed state occurs only when there is a movement of the right hand (see Fig. 8).

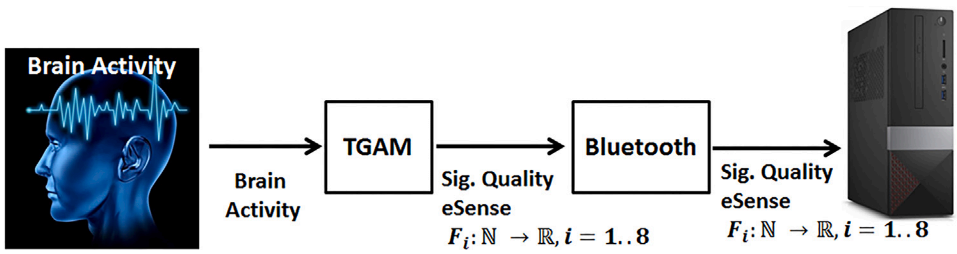


**Fig. 6.** Overview of the system's processing pipeline.

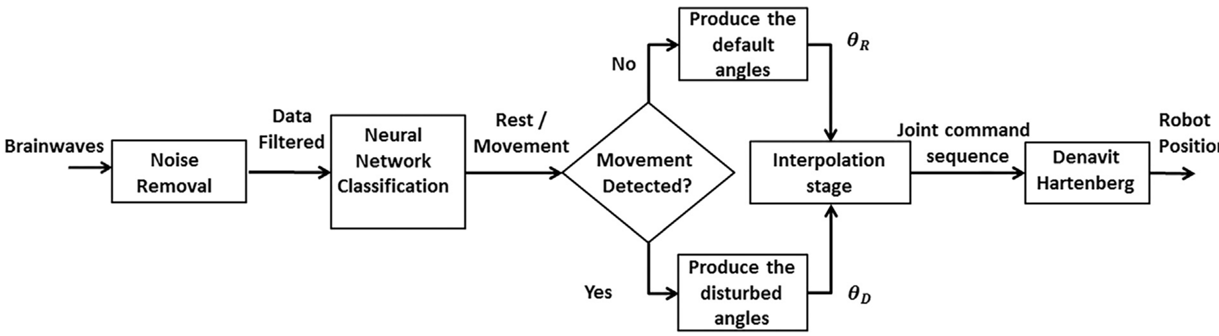


**Fig. 7.** Translation of brain signal to movement.

(a) Hand in rest state (b) Hand in disturbed state

**Fig. 8.** Angular position of the finger joints in each state.

The pre-trained NN classifies the data and verifies whether or not there is elementary movement in the analyzed data. If there is no movement, the predefined rest angles are produced ($\theta_R = [\theta_{r1}\ \theta_{r2}]$), whereas if there is any movement, the disturbance predefined angles are produced ($\theta_D = [\theta_{d1}\ \theta_{d2}]$). The next stage makes the interpolation in $N$steps between the current robot joints angles and the angles fed to it, this stage makes the binary and aggressive movement become a smoothing movement. The sequence of angles is fed to the DH model, which executes the command and changes the position of the robot.

## 4. Results and discussions

### 4.1. Data collected

The implemented system was developed using five brain activity recorded series of the same subject. The headset provides ten different signals, Signal Quality, Attention, Meditation, Delta, Theta, Low Alpha, High Alpha, Low Beta, High Beta, Low Gamma, and Mid Gamma brainwaves, among these signals, only the brainwaves that belong to the sensorimotor rhythms (Alpha and Beta brainwaves) were used.

Fig. 9 shows the signals from dataset 1, it is a plot with 1818 samples, each one spent a second to be recorded, so the entire dataset is approximately thirty minutes, which shows that the first dataset is composed of the three ten-minute sections grouped in sequence. This dataset will be used to train the NN. The second dataset will be used to test and validate the NN, it was composed of two recorded two-minute series with 238 samples (see Table 7).

**Table 7**
$N_{OM}$: The number of the samples with others movements of the dataset 2. $N_{NM}$: The number of the samples with no movements of the dataset 2. $N_{OM} + N_{NM} = 119$.

| | Samples with elementary movement | Samples with others movements | Samples with no movement |
|---|---|---|---|
| Dataset 1 | 606 | 606 | 606 |
| Dataset 2 | 119 | $N_{OM}$ | $N_{NM}$ |

### 4.2. Noise removal

The EEG signal depicted in Fig. 9 exhibits significant noise, necessitating the use of a filter to eliminate or reduce high-frequency interference and make the signal more suitable for classification. The Moving Average (MA) filter was chosen because it is a good type of FIR (Finite Impulse Response) filter, that is, its output is always the average of $N$ samples of the input signal, besides presenting a linear phase, which means, the result that all frequency components of the input signal are shifted in time by the same constant amount.

The MA filter was used twice with the same window length to increase the smoothness and eliminate the noise from brainwave signals. Fig. 10 illustrates the filtered brainwave signals, the frequency bands $F_i(k)\ \mathbb{N} \rightarrow \mathbb{R},\ i = 3..6$ (Low Alpha, High Alpha, Low Beta, High Beta) correspond to Low Alpha, High Alpha, Low Beta, and High Beta. The main disadvantage of this filter is the time delay associated with the length of the filter window, as demonstrated in Fig. 11. This can be a problem in a real-time data processing if the delay time is bigger than the period of a specific event of the signal, which becomes impossible to get this characteristic, another problem related to the loss of information is using the filter many times in the same signal, which causes a super smoothing in the data, which result in loss of own characteristics and, consequently, in the loss of information.

The more the filter is used on the same data, the smoother it becomes, but it does not greatly influence the time delay. The length of the filter window is sixteen samples, and each sample takes one second to be recorded, so the delay time for this filtering is fifteen seconds,

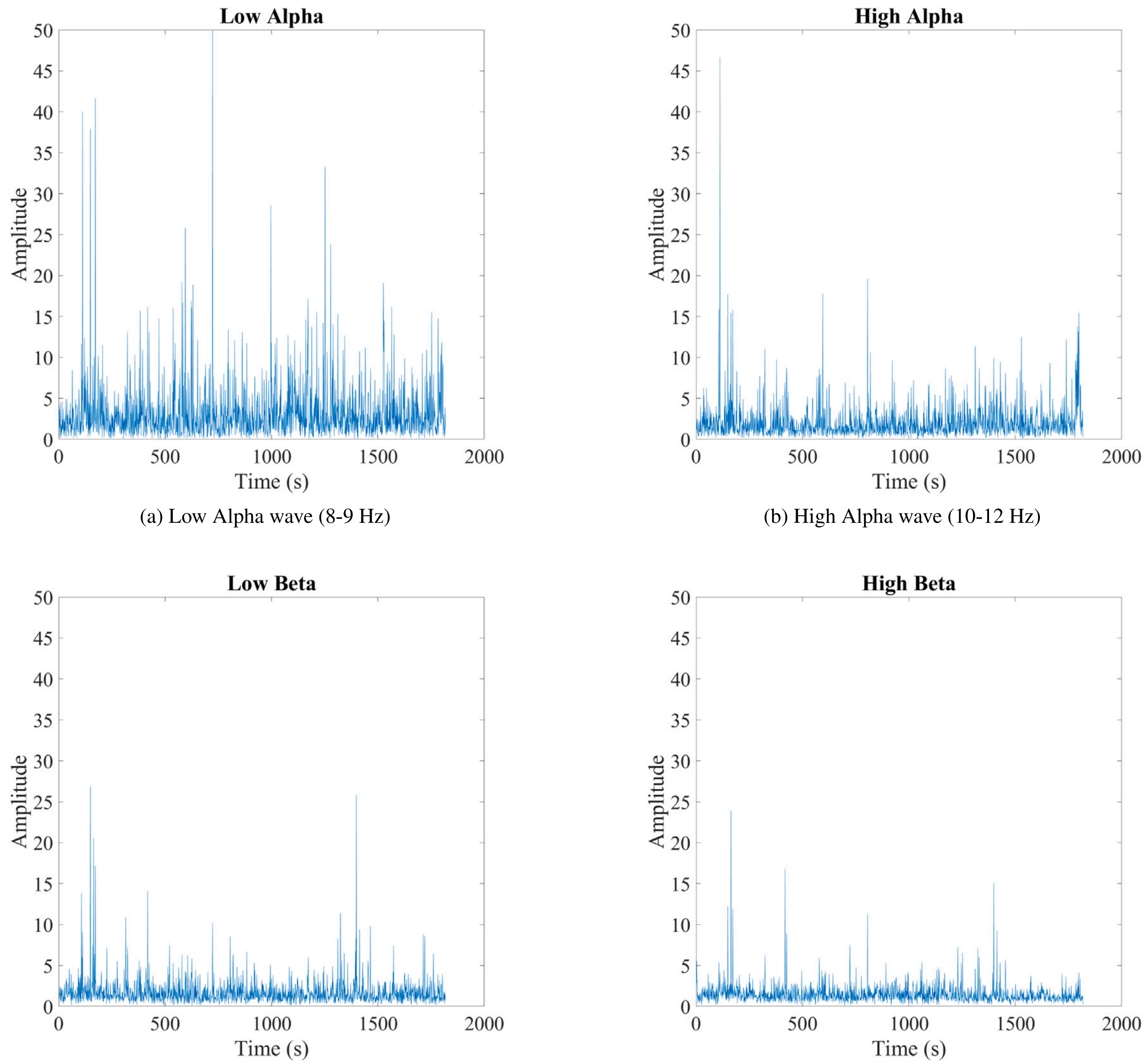


(a) Low Alpha wave (8-9 Hz)

(b) High Alpha wave (10-12 Hz)

(c) Low Beta wave (13-17 Hz)

(d) High Beta wave (18-30 Hz)

**Fig. 9.** Used brainwaves.

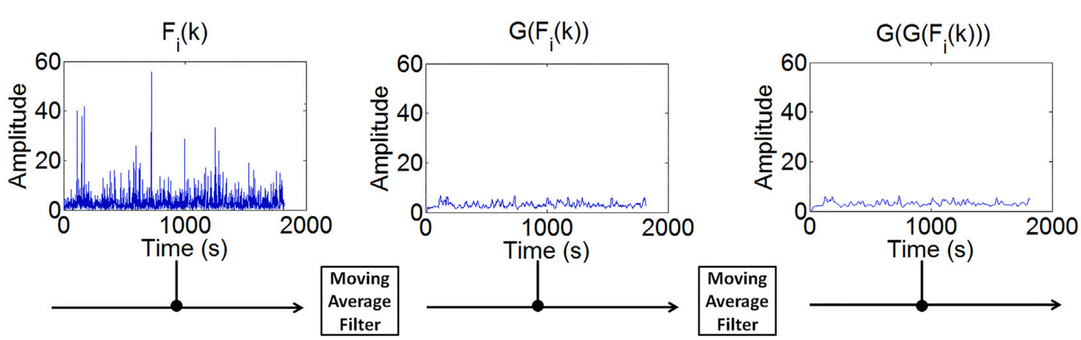


**Fig. 10.** Filtered brainwaves.

ie it is necessary to wait fifteen seconds/samples to get the first data smoothed.

### 4.3. Neural network

The sequential grouping of the dataset led to overfitting in the Multilayer Perceptron (MLP) neural network. This issue caused the network to fit the previously observed dataset extremely well but fail to generalize when predicting new results. To mitigate this problem, the dataset was randomly shuffled using a custom sorting function developed in MATLAB™. Since the training process is supervised, this reorganization does not compromise the learning process.

A Multilayer Perceptron (MLP) neural network consists of three layers: input, hidden, and output. The input layer contains neurons that receive the input data, the hidden layers contain neurons responsible for learning more complex representations, and the output layer contains neurons responsible for generating the network's output.

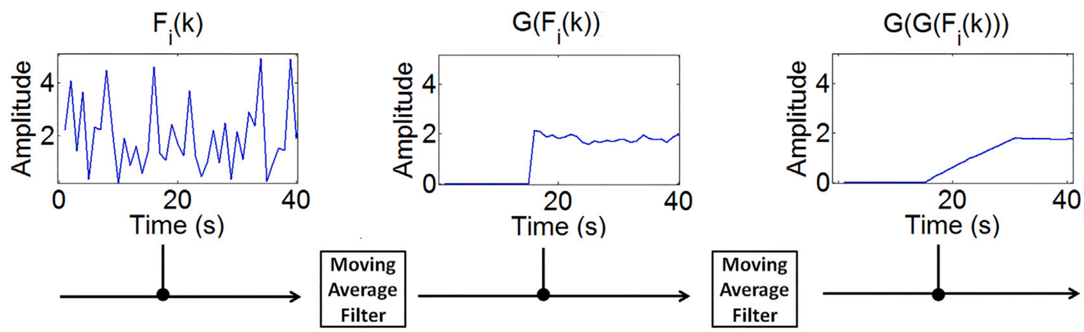


**Fig. 11.** Delay caused by the Moving Average Filter.

The MLP is one of the most common feed-forward artificial neural networks [33], inspired by the way the human brain processes information. The MLP consists of an input layer, one or more hidden layers, and an output layer, with each hidden layer fully connected to the subsequent layer. The hidden layers are used to perform nonlinear mapping on the input space, and the output layer is used to generate the classification results. The output of each neuron in the hidden layer is the weighted sum of the input signals, which are multiplied by their respective connection weights and then passed through an activation function, as defined in Eq. (4):

$$y_j = f\left(\sum w_{ij} x_i + b_i\right) \tag{4}$$

Where $f$ is an activation function, $b_i$ denotes a bias term, and $w_{ij}$ represents the connection weight from the $i$-th neuron of the previous layer to the $j$-th neuron of the current layer.

For the activation function, we use the most commonly applied type, the hyperbolic tangent function, which has been widely used in previous studies. It is defined in Eq. (5):

$$\tanh(x) = \frac{\exp(x) - \exp(-x)}{\exp(x) + \exp(-x)} \tag{5}$$

After filtering and reordering, the data were used as inputs for the MLP, which was trained using multiple configurations of layers and neurons. The Broyden–Fletcher–Goldfarb–Shanno (BFGS) Quasi-Newton backpropagation algorithm ('trainbfg') was employed for training. This second-order optimization method is more efficient than standard gradient descent as it approximates the Hessian matrix to accelerate convergence. The BFGS update is defined in Eq. (6), [34].

$$H_{t+1} = H_t + \frac{y^t \otimes y^t}{\langle y^t, s^t\rangle} - \frac{(H_t s^t) \otimes (H_t s^t)}{\langle s^t, H_t, s^t\rangle} \tag{6}$$

A key property of BFGS is that $H_t$ is always positive definite, ensuring no regularization is needed. Additionally, assuming that $f$ is a strongly convex quadratic function with Hessian $A$, BFGS applied to $f$ with a perfect line search and any positive definite initial guess for $H_0$ satisfies $H_p = A$, meaning the method recovers the true curvature of the function in finite time. In a general setting, under mild assumptions, BFGS also achieves the desired quadratic convergence.

The goal of the learning process is to minimize the error rate of the network's output when compared to the ground truth [33]. The cross-entropy loss function ('crossentropy') was used to evaluate the network's performance. This function is particularly suitable for classification tasks, as it measures the divergence between the predicted probability distribution and the actual class labels, penalizing incorrect classifications. The function is defined in Eq. (7):

$$\sum_{c=1}^{M} y_{o,c} \log(p_{o,c}) \tag{7}$$

Where $M$ is the number of classes (2 for this article, representing the presence or absence of the elementary movement), $y$ is a binary indicator of whether the prediction that class $c$ is the class of observed data $o$ is correct, and finally, $p$ is the probability that the aforementioned data $o$ belongs to the class label $c$.

**Table 8**
Some architectures tested in training stage.

| Architecture | Number of neurons in each layer | Accuracy dataset 1 (Training dataset) |
|---|---|---|
| 1 | 18\|12\|5 | 99, 30% |
| 2 | 25\|18 | 99, 50% |
| 3 | 18\|5\|12 | 94, 40% |
| 4 | 14\|10\|6\|5 | 96, 10% |
| 5 | 4\|8\|12\|14 | 99, 00% |
| 6 | 24\|21 | 99, 70% |

To determine the optimal MLP configuration, multiple networks with different numbers of hidden layers and neurons per layer were trained. The results of this process are summarized in Table 8, which presents the performance of various configurations. Among the tested architectures, configurations 2 and 6 were selected for further validation using a second dataset, as they demonstrated superior accuracy and better generalization capabilities, minimizing the risk of overfitting. The NN classification errors of the selected architectures are represented by confusion matrices in Table 9. In these matrices, the rows correspond to the predicted (output) class, while the columns correspond to the true (target) class. Here, 1 indicates detected movement, and 2 indicates other or no movement.

In the field of machine learning, the confusion matrix or error matrix is a specific table layout that allows the visualization of the performance of an algorithm. The matrix shows the positive instances in green cells and the negative instances in the red cells. The matrix order is related to how many kinds of targets there are in the dataset, that is, the matrix is composed only of the green and red cells, e.g., the datasets used in this research have two classes, the first is the class that contain the elementary movement, and the other is the class that does not contain this information, so there are two targets, then the matrix is of order two.

The white and blue cells are related to the performance of the algorithm. The percentages in the white cells of the rows represent the precision of the NN output, i.e., how many predicted samples in each class were correctly and incorrectly sorted, while the percentage in the white cells of the columns represents the precision of the target class, i.e. how many samples of each class (1,2) were classified correctly and incorrectly. The blue cell represents the overall accuracy of the NN.

When comparing the two matrices, it is notable that architecture 2 has the best result, that is, this architecture can predict new results better than the other. An accuracy rate of 73, 9% is an acceptable result that confirms the usability of the single-channel headset to make BCI solutions.

The system output is shown in Fig. 12. Using a single electrode on the forehead, it was possible to extract the motor information even though the electrode was not located in the area of the motor cortex, this was possible because the brain waves are a sum of the firing of the neurons.

**Table 9**
NN classification errors of architectures 2 and 6.

Correct rating | Wrong rating | Partial accuracy | Overall accuracy

**Confusion Matrix: Architecture 2**

| Output Class \ Target Class | 1 | 2 | |
|---|---|---|---|
| 1 | 60 (25.2%) | 3 (1.3%) | 95.2% 4.8% |
| 2 | 59 (24.8%) | 116 (48.7%) | 66.3% 33.7% |
| | 50.4% 49.6% | 97.5% 2.5% | 73.9% 26.1% |

**Confusion Matrix: Architecture 6**

| Output Class \ Target Class | 1 | 2 | |
|---|---|---|---|
| 1 | 38 (16.0%) | 2 (0.8%) | 95.0% 5.0% |
| 2 | 81 (34.0%) | 117 (49.2%) | 59.1% 40.9% |
| | 31.9% 68.1% | 98.3% 1.7% | 65.1% 34.9% |

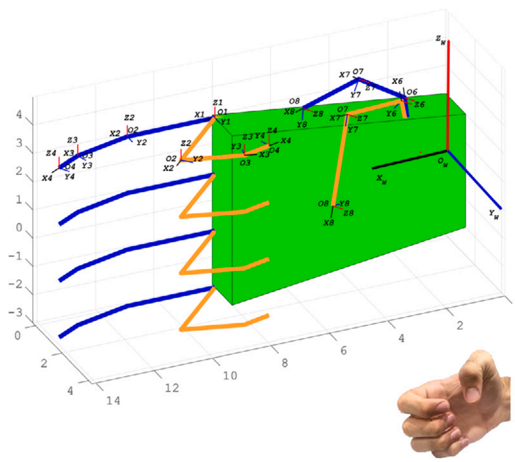

**Fig. 12.** Hand (DH) movement after NN data classification.

### 4.4. Discussion of limitations

The use of data from a single subject might restrict the generalizability and robustness of the model. Although the accuracy achieved of 80.7% in detecting right-hand movement is promising, the results cannot be fully extrapolated to a broader population without further validation. Furthermore, the current system's reaction time of 15 s is not suitable for real-time applications, highlighting the need for optimization to improve responsiveness.

Future work will address these limitations by expanding experiments to include multiple subjects with diverse demographics and neurological conditions. This will help evaluate the model's adaptability and reliability across different users. Despite these current limitations, the source code is publicly available[1] to facilitate reproducibility and enable further research, encouraging adaptation and building upon this work according to specific needs.

## 5. Conclusion

The goal of extracting information from the motor cortex with a single-channel headset and translating it into a robot movement was reached. The success in extracting the information shows the possibility of detecting the movement-intention. The results obtained do not allow produce useful neuroprostheses but show a real path of study and development to make cheaper and accessible solutions.

The main disadvantage of the developed system in real time, it is the delay time caused by the filtering of the signal. To improve the results and closer this experiment a useful solution, a must be do a study in the extraction of the movement intention from the brainwaves with the used headset.

The datasets must be increased to get more data to use in the training and validation stage of the NN to get a better result of the classifier. The noise removal stage must use real-time filters, to eliminate or reduce the time delay to allow the use in real-time situations. The way of receiving the data must change to eliminate the step of recording the brainwaves in a .txt file and do direct communication with the MATLAB code, allowing simultaneous data processing.

As future work, we also plan to explore techniques to reduce reaction time, such as optimizing the neural network architecture and implementing more efficient signal processing algorithms. By standardizing the training protocol and testing in varied experimental settings, we aim to establish a robust framework for developing cost-effective and accessible neural prostheses, paving the way for real-world applications of Brain–Computer Interface systems.

## CRediT authorship contribution statement

**A.B.R. Lara:** Writing – original draft, Validation, Methodology, Investigation, Formal analysis, Data curation, Conceptualization. **Oscar E. Ruiz:** Writing – original draft, Supervision. **L.O. Araujo Junior:** Writing – original draft, Conceptualization. **F.P. Bhering:** Writing – original draft, Supervision.

## Declaration of competing interest

The authors declare the following financial interests/personal relationships which may be considered as potential competing interests: Fabiano Pereira Bhering reports financial support was provided by Federal Technological Education Centre of Minas Gerais. If there are other authors, they declare that they have no known competing financial interests or personal relationships that could have appeared to influence the work reported in this paper.

## Data availability

Link to a publicly available repository containing our source code in Manuscript.

## References

[1] Jacques J. Vidal, Toward direct brain-computer communication, Annu. Rev. Biophys. Bioeng. 2 (1) (1973) 157–180.
[2] Babak A. Taheri, Robert T. Knight, Rosemary L. Smith, A dry electrode for EEG recording, Electroencephalogr. Clin. Neurophysiol. 90 (5) (1994) 376–383.
[3] Hongqi Li, Xiaoya Li, José del R. Millán, Noninvasive EEG-based intelligent mobile robots: A systematic review, IEEE Trans. Autom. Sci. Eng. (2024).
[4] Roberto Portillo-Lara, Bogachan Tahirbegi, Christopher AR Chapman, Josef A Goding, Rylie A Green, Mind the gap: State-of-the-art technologies and applications for EEG-based brain–computer interfaces, APL Bioeng. 5 (3) (2021).

[1] https://github.com/ABLara/BrainWaves.git

[5] Janis Peksa, Dmytro Mamchur, State-of-the-art on brain-computer interface technology, Sensors 23 (13) (2023) 6001.
[6] Rahul Ajmeria, Mayukh Mondal, Reya Banerjee, Tamesh Halder, Pallav Kumar Deb, Debasish Mishra, Pravanjan Nayak, Sudip Misra, Surjya Kanta Pal, Debashish Chakravarty, A critical survey of eeg-based bci systems for applications in industrial internet of things, IEEE Commun. Surv. & Tutorials 25 (1) (2022) 184–212.
[7] Mohamad Amlie Abu Kasim, Cheng Yee Low, Muhammad Azmi Ayub, Noor Ayuni Che Zakaria, Muhammad Haszerul Mohd Salleh, Khairunnisa Johar, Hizzul Hamli, User-friendly LabVIEW GUI for prosthetic hand control using emotiv EEG headset, Procedia Comput. Sci. 105 (2017) 276–281.
[8] Rashima Mahajan, Dipali Bansal, Real time EEG based cognitive brain computer interface for control applications via arduino interfacing, Procedia Comput. Sci. 115 (2017) 812–820.
[9] Justin Kilmarx, Reza Abiri, Soheil Borhani, Yang Jiang, Xiaopeng Zhao, Sequence-based manipulation of robotic arm control in brain machine interface, Int. J. Intell. Robot. Appl. 2 (2) (2018) 149–160.
[10] Harun Çiğ, Davut Hanbay, Fatih Tüysüz, Robot arm control with for SSVEP-based brain signals in brain computer interface, in: Artificial Intelligence and Data Processing Symposium (IDAP), 2017 International, IEEE, 2017, pp. 1–6.
[11] Esmeralda Contessa Djamal, Dimas Andhika Sury, Multi-channel of electroencephalogram signal in multivariable brain-computer interface, IAES Int. J. Artif. Intell. 12 (2) (2023) 618.
[12] Catharina Zich, Maarten De Vos, Cornelia Kranczioch, Stefan Debener, Wireless EEG with individualized channel layout enables efficient motor imagery training, Clin. Neurophysiol. 126 (4) (2015) 698–710.
[13] Lei Cao, Jie Li, Hongfei Ji, Changjun Jiang, A hybrid brain computer interface system based on the neurophysiological protocol and brain-actuated switch for wheelchair control, J. Neurosci. Methods 229 (2014) 33–43.
[14] Dennis J. McFarland, William A. Sarnacki, Jonathan R. Wolpaw, Electroencephalographic (EEG) control of three-dimensional movement, J. Neural Eng. 7 (3) (2010) 036007.
[15] Daniel Pérez-Marcos, Jaime Alberto Buitrago, Fáber Danilo Giraldo Velásquez, Writing through a robot: A proof of concept for a brain–machine interface, Med. Eng. Phys. 33 (10) (2011) 1314–1317.
[16] C. Nandagopal, B. Sneha, R. Sriragavi, R. Veeradharshini, Brainwave sensor based smart home controller for paralysed people, in: 2023 International Conference on Sustainable Computing and Data Communication Systems, ICSCDS, IEEE, 2023, pp. 801–807.
[17] Siliveru Ramesh, M. Gopi Krishna, Madhu Nakirekanti, Brain computer interface system for mind controlled robot using bluetooth, Int. J. Comput. Appl. 104 (15) (2014).
[18] Devashish Salvekar, Amrita Nair, Dany Bright, SA Bhisikar, Mind controlled robotic arm, IOSR J. Electron. Commun. Engineering (IOSR- JECE) (2015) 36–44.
[19] Dany Bright, Amrita Nair, Devashish Salvekar, Swati Bhisikar, EEG-based brain controlled prosthetic arm, in: Advances in Signal Processing (CASP), Conference on, IEEE, 2016, pp. 479–483.
[20] Rahul Raj, Suman Deb, Paritosh Bhattacharya, Brain computer interfaced single key omni directional pointing and command system: a screen pointing interface for differently-abled person, Procedia Comput. Sci. 133 (2018) 161–168.
[21] Qi Xu, Hui Zhou, Yongji Wang, Jian Huang, Fuzzy support vector machine for classification of EEG signals using wavelet-based features, Med. Eng. Phys. 31 (7) (2009) 858–865.
[22] Roberto Munoz, et al., Analysis and classification of electroencephalographic signals (EEG) to identify arm movements, in: Electrical Engineering, Computing Science and Automatic Control (CCE), 2013 10th International Conference on, IEEE, 2013, pp. 138–143.
[23] Jian-Zhong Xue, Hui Zhang, Chong-Xun Zheng, Xiang-Guo Yan, Wavelet packet transform for feature extraction of EEG during mental tasks, in: Machine Learning and Cybernetics, 2003 International Conference on, vol. 1, IEEE, 2003, pp. 360–363.
[24] Kouhyar Tavakolian, Ali Motie Nasrabadi, Siamak Rezaei, Selecting better EEG channels for classification of mental tasks, in: Circuits and Systems, 2004. ISCAS'04. Proceedings of the 2004 International Symposium on, vol. 3, IEEE, 2004, pp. III–537.
[25] Swati Rajwal, Swati Aggarwal, Convolutional neural network-based EEG signal analysis: A systematic review, Arch. Comput. Methods Eng. 30 (6) (2023) 3585–3615.
[26] Hamdi Altaheri, Ghulam Muhammad, Mansour Alsulaiman, Syed Umar Amin, Ghadir Ali Altuwaijri, Wadood Abdul, Mohamed A Bencherif, Mohammed Faisal, Deep learning techniques for classification of electroencephalogram (EEG) motor imagery (MI) signals: A review, Neural Comput. Appl. 35 (20) (2023) 14681–14722.
[27] Wenjia Ouyang, Kelly Cashion, Vijayan K. Asari, Electroencephelograph based brain machine interface for controlling a robotic arm, in: Applied Imagery Pattern Recognition Workshop (AIPR): Sensing for Control and Augmentation, 2013 IEEE, IEEE, 2013, pp. 1–7.
[28] Malgorzata Plechawska-Wojcik, Piotr Wolszczak, Radoslaw Cechowicz, Krystian Łygas, Construction of neural nets in brain-computer interface for robot arm steering, in: Human System Interactions (HSI), 2016 9th International Conference on, IEEE, 2016, pp. 348–354.
[29] Elliott M. Forney, Charles W. Anderson, Classification of EEG during imagined mental tasks by forecasting with elman recurrent neural networks, in: Neural Networks (IJCNN), the 2011 International Joint Conference on, IEEE, 2011, pp. 2749–2755.
[30] Yoram Koren, Yoram Koren, Robotics for Engineers, vol. 168, McGraw-Hill New York et al, 1985.
[31] Gert Pfurtscheller, F.H. Lopes Da Silva, Event-related EEG/MEG synchronization and desynchronization: basic principles, Clin. Neurophysiol. 110 (11) (1999) 1842–1857.
[32] Gert Pfurtscheller, A. Aranibar, Event-related cortical desynchronization detected by power measurements of scalp EEG, Electroencephalogr. Clin. Neurophysiol. 42 (6) (1977) 817–826.
[33] Jordan J. Bird, Jhonatan Kobylarz, Diego R. Faria, Anikó Ekárt, Eduardo P. Ribeiro, Cross-domain MLP and CNN transfer learning for biological signal processing: EEG and EMG, IEEE Access 8 (2020) 54789–54801, http://dx.doi.org/10.1109/ACCESS.2020.2979074.
[34] Pierre Ablin, Exploration of multivariate EEG /MEG signals using non-stationary models (Ph.D. thesis), (2019SACLT051) Université Paris Saclay (COmUE), 2019, URL https://pastel.hal.science/tel-02507788.